

# Durability and physical characterization of anti-fogging solution for 3D-printed clear masks and face shields

Succhay Gadhar<sup>Equal first author, 1</sup>, Shaina Chechang<sup>Equal first author, 1</sup>, Philip Sales<sup>1</sup>, Praveen Arany<sup>Corresp. 1</sup>

<sup>1</sup> Oral Biology, Biomedical Engineering, and Surgery, University at Buffalo, Buffalo, NY, USA

Corresponding Author: Praveen Arany  
Email address: praveenarany@gmail.com

**Background.** The COVID-19 pandemic brought forth the crucial roles of personal protective equipment (PPE) such as face masks and shields. Additive manufacturing with 3D printing enabled customization and generation of transparent PPEs. However, these devices were prone to condensation from normal breathing. This study was motivated to seek a safe, non-toxic, and durable anti-fogging solution. **Methods.** We used additive 3D printing to generate the testing apparatus for contact angle, sliding angle, and surface contact testing. We examined several formulations of carnauba wax to beeswax in different solvents and spray-coated them on PETG transparent sheets for testing contact and sliding angle, and optical clarity. Further, the integrity of this surface following several disinfection methods such as soap, Isopropyl Alcohol, or water alone with gauze, paper towels, and microfiber, along with disinfectant wipes, was assessed. **Results.** The results indicate a 1 : 2 ratio of carnauba to beeswax in Acetone optimally generated a superhydrophobic surface (contact angle  $150.3 \pm 2.1^\circ$  and sliding angle  $13.7 \pm 2.1^\circ$ ) with maximal optical clarity. The use of soap for disinfection resulted in the complete removal of the anti-fogging coating, while Isopropyl Alcohol and gauze optimally maintained the integrity of the coated surface. Finally, the contact surface testing apparatus generated a light touch ( $5000 \text{ N/m}^2$ ) that demonstrated good integrity of the antifogging surface. These results suggest that the routine use of clear PPEs could be further enabled by using a novel anti-fogging solution.

1     **Durability and Physical Characterization of Anti-Fogging**  
2     **Solution for 3D-Printed Clear Masks and Face Shields**

3             Succhay Gadhar<sup>1,\*</sup>, Shaina Chechang<sup>1,\*</sup>, Philip Sales<sup>1</sup>, Praveen R. Arany<sup>1,\$</sup>

4             <sup>1</sup> Oral Biology, Biomedical Engineering and Surgery, University at Buffalo, NY, USA

5     \* Equal contributions

6

7     <sup>\$</sup>**Address correspondence to:**

8     Praveen R. Arany B.D.S., M.D.S., M.M.Sc., Ph.D.

9     3435 Main Street, BRB 553,

10    Buffalo, NY 14214.

11    E-mail: [prarany@buffalo.edu](mailto:prarany@buffalo.edu)

12    Phone: 716-829-3479

13

14

15    **Keywords:** Face shields, Masks, Anti-fogging

16

17

18

19 **ABSTRACT**

20 **Background.** The COVID-19 pandemic brought forth the crucial roles of personal protective  
21 equipment (PPE) such as face masks and shields. Additive manufacturing with 3D printing enabled  
22 customization and generation of transparent PPEs. However, these devices were prone to  
23 condensation from normal breathing. This study was motivated to seek a safe, non-toxic, and  
24 durable anti-fogging solution.

25 **Methods.** We used additive 3D printing to generate the testing apparatus for contact angle, sliding  
26 angle, and surface contact testing. We examined several formulations of carnauba wax to beeswax  
27 in different solvents and spray-coated them on PETG transparent sheets for testing contact and  
28 sliding angle, and optical clarity. Further, the integrity of this surface following several disinfection  
29 methods such as soap, Isopropyl Alcohol, or water alone with gauze, paper towels, and microfiber,  
30 along with disinfectant wipes, was assessed.

31 **Results.** The results indicate a 1 : 2 ratio of carnauba to beeswax in Acetone optimally generated  
32 a superhydrophobic surface (contact angle  $150.3 \pm 2.1^\circ$  and sliding angle  $13.7 \pm 2.1^\circ$ ) with  
33 maximal optical clarity. The use of soap for disinfection resulted in the complete removal of the  
34 anti-fogging coating, while Isopropyl Alcohol and gauze optimally maintained the integrity of the  
35 coated surface. Finally, the contact surface testing apparatus generated a light touch ( $5000 \text{ N/m}^2$ )  
36 that demonstrated good integrity of the antifogging surface. These results suggest that the routine  
37 use of clear PPEs could be further enabled by using a novel anti-fogging solution.

38

39

40

41

42

43

44

45

46

47 **INTRODUCTION**

48           The COVID-19 pandemic has had a significant toll on the public health, biomedical, and  
49 financial aspects that have significantly changed society.(1,2) Among various healthcare services,  
50 the presence of SARS-CoV in the nasal and upper respiratory tract presented significant challenges  
51 for dentists and anesthetists. Clinical dentistry presented a significant challenge due to the  
52 proximity and inherent aerosol-generating procedures. (3-5) The use of personal protection  
53 equipment (PPE) such as face masks and face shields was integral in reducing the spread of  
54 infections among the general population. (6) While dentistry routinely utilizes face masks, double  
55 masking, and the impervious nature of N95 further compounded the pandemic fear and anxiety in  
56 patients naturally apprehensive about their dental visits. (7-9) Another major limitation of these  
57 masks is that they hindered communication due to the lack of non-verbal cues such as facial  
58 expressions, lip and tongue movements. (10-12) This is particularly challenging in differentially  
59 ables (hearing impaired) patients due to voice attenuation with increased ambient noise in dental  
60 operatories. (13-16) The use of transparent masks and face shields has been demonstrated to  
61 improve these limitations. (17)

62           Another major challenge during the early phase of the pandemic was the significant  
63 disruption of the PPE supply chain requiring local innovations where additive manufacturing using  
64 3D printing came to the forefront. (18-21) The ability to generate required quantities based on need  
65 and additional customization for individual applications were significant advantages of this  
66 approach. (22) Building on this, in collaboration with e-NABLE, a 3D printing community,  
67 students at the University at Buffalo School of Dental Medicine generated transparent PPEs using  
68 3D printing and vacuum casting. Among them, several custom designs were specifically generated  
69 to accommodate commercially available dental loupes that are made available freely online.(23)  
70 These clear masks and face shields were well accepted and generated much enthusiasm among  
71 clinical users. Besides dentistry, another group of clinicians that notably adopted these clear PPEs  
72 were the local speech and hearing-impaired clinics. However, an immediate limitation of this  
73 approach reported by users was the fogging due to the moisture from regular breathing. This  
74 essentially negated the advantage of the transparent nature of these masks and face shields and  
75 presented additional hindrance of needing repetitive wipe-downs.

76           The commercially available anti-fogging solutions used for eyeglasses and car exteriors  
77 contain polydimethylsiloxane and silica nanoparticles. The long-term use of these solutions was  
78 considered unsuitable due to their potential for skin irritation, and potential inhalation or ingestion.  
79 Hence, we sought to identify a non-toxic, antifogging coating for the transparent masks and face  
80 shields for long-term use. To design such a solution, specific design criteria needed to be met. The  
81 surface of a water droplet is attracted to the bulk of the droplet due to cohesion which results in  
82 their beading. The shape that a drop takes on a given surface depends on the surface tension of the  
83 fluid and the physical characteristics of the surface. A surface-fluid interface is the contact angle  
84 that measures the wettability of a surface. Contact angles can vary from hydrophilic (less than or  
85 equal to  $30^\circ$ ), hydrophobic ( $120^\circ$ ), or superhydrophobic (over  $150^\circ$ ) where the higher the contact  
86 angle, the lower its wettability. (24) Another measure of the extent of moisture retention on a  
87 surface is the sliding angle which is measured by tilting the surface with the solution bead to  
88 determine the angle at which it rolls off. The more hydrophobic the surface, the higher the angle  
89 of loss of fluid droplets.(25) Another key design aspect of the anti-fogging solution would be its  
90 resistance to wear due to repeated skin surface contact during mask use. The ideal solution would  
91 offer a thin, durable coating for daily use that would not need repetitive applications while  
92 maintaining maximal transparency.

93           Natural products offer attractive non-toxic coatings. Prior studies have examined the  
94 combination of cinnamon and nutmeg that produces high hydrophobicity. (26) Although both are  
95 natural products, there are some toxicity concerns due to high cuprous oxide. Drawing inspiration  
96 from the naturally-occurring, extremely hydrophobic lotus leaves that expel water due to their  
97 micro-structural features termed papillae that exude epicuticular waxes, cutin. (27,28)  
98 Alternatively, Carnauba and beeswax have also been shown to achieve high hydrophobicity. (29)  
99 With high hydrophobicity, the solution was intended for food containers to prevent waste.  
100 However, there was a lack of clarity in the concentrations used and the resulting hydrophobicity.  
101 This study examined the different formulations of these two waxes together and evaluated the  
102 contact angle, sliding angle, and optical clarity. The optimized formulation was subjected to  
103 durability testing with manual disinfectant procedures and long-term contact-wear testing.

104

105

## 106 MATERIALS AND METHODS

### 107 Formulation of anti-fogging solutions

108 Hydrophobic wax coatings were generated in acetone or methanol as solvents using  
109 ultrasonication. Different ratios of carnauba wax to beeswax were employed namely 0.4375 g:  
110 0.4375 g (1:1), 0.35 g: 0.525 g (1:1.5), 0.33 g: 0.66 g (1:2), 0.417 g: 0.834 g (1:2) were melted in  
111 a 50 ml plastic tube (Corning, Thermofisher Waltham, MA) in a water bath. After the waxes had  
112 melted, 25 milliliters of either acetone or methanol (both Sigma Aldrich, St. Louis, MO) were  
113 added, and the solution was emulsified immediately using ultrasonication (Q2000, QSonica,  
114 Newtown CT) at 90% amplitude for 3 minutes and transferred into a 2 oz glass spray bottle.

### 115 Contact and Sliding Angle testing

116 Solutions were sprayed onto a 2 x 2-inch sheet of PETG at roughly a distance of 5 inches, spraying  
117 10 times. After drying, the sheets of PETG were tested for contact angle, sliding angle, and  
118 transmission. A custom contact and sliding angle device were generated based on commercially  
119 available models using online CAD software (Onshape, PTC, Rockwell Automation, Boston MA).  
120 The devices were printed using Polylactic acid (PLA) filament (Overture, Overture 3D  
121 Technologies, Texas) on a i3 Prusa 3D printer (Prussa Research, Prague Czech Republic) (**Figs. 1**  
122 **A - C**). The device included a slot for to hold a mobile phone to take digital pictures of the droplet.  
123 After fixing the plastic surface to the platform, droplets of water were generated with a 3 ml syringe  
124 and 14-gauge needle and digital image were captured for analysis (**Fig. 1 D**). The digital images  
125 were analyzed using the NIH ImageJ (ver. 1.53n) software. The sliding angle set up included a  
126 protractor to assess the angle at which the droplet slides off. The platform was tilted slowly until  
127 the water droplet slid off, and the angle was documented (**Fig. 1 E**). All studies were performed in  
128 replicated and repeated at least twice.

### 129 Optical clarity analysis

130 The laser apparatus consisted of a 650 nm diode laser (Weber Medical, Beverungen, Germany) at  
131 10 mW/cm<sup>2</sup>, and a sensor with power meter (both Thor Labs, Newton NJ) (**Fig. 1F**). The sheets  
132 of PETG were placed on top of the power sensor, and transmission was assessed.

133

**134 Routine manual disinfection testing**

135 The PETG coated surfaces were subjected to different solutions such as soap solution (10% v/v,  
136 Dawn, Procter & Gamble, Cincinnati OH), Isopropyl alcohol (70%, Sigma Aldrich, St. Louis MO),  
137 and water alone using paper towels (Uline, Milton ON), gauge (Henry Schein, New York, NY) or  
138 microfibers (Magic Fiber, Miami FL). These disinfectants were applied ten times in a uniform,  
139 lateral motion with constant manual pressure by a single operator. Disinfection wipes (Metrex,  
140 Orange CA) were used in another group.

**141 Coating Durability following contact wear testing**

142 To simulate accelerated contact wear testing, a custom apparatus was designed to mimic skin  
143 contact. Using the CAD software (Onshape, PTC, Rockwell Automation, Boston MA), a rotating  
144 platform with spring-loaded bases was designed to apply suitable skin contact forces. (30-32) The  
145 device was 3D printed with PLA filament (Overture, Overture 3D Technologies, Texas) on a i3  
146 Prusa 3D printer (Prusa Research, Prague Czech Republic). The wheel was connected to a DC  
147 Motor (Greartisan, Shenzhen Hotec, China) via a speed controller and a 9V battery which allowed  
148 the motor to function up to 1000 RPMs. After the coated samples were mounted on the platforms,  
149 the apparatus was positioned to allow the platforms to extend and retract using centrifugal force  
150 while spinning, hitting a skin-equivalent surface to simulate contact. To simulate multiple skin  
151 contacts, the device was operated for 5 minutes, allowing each platform to contact the wall about  
152 5000 times for each sample. The contact force applied by the rotational, spring-loaded platform  
153 was measured with a digital force probe (Baoshishan, China). Following the contact wear testing,  
154 samples were assessed for changes in contact angle, sliding angle, optical clarity and examined  
155 with ultrastructure analysis.

**156 Ultrastructure analysis**

157 Scanning electron microscopy (SEM) analysis was performed to determine the coating on the  
158 plastic sheet samples. Samples were sputter-coated for 120 seconds and examined using SEM  
159 (Hitachi, S-4700, Japan) with a voltage of 15 kV.

160

161

## 162 **Statistical Analysis**

163 Data was organized in Excel (Microsoft, Seattle WA) and presented as Means with standard  
164 deviations. Data was subjected to a student T test was performed or two-way analysis of variance  
165 (ANOVA) among different treatments with Bonferroni's correction for multiple comparisons  
166 where appropriate. A  $p < 0.05$  was considered statistically significant.

167

## 168 **RESULTS**

### 169 **Formulation and Characterization of Anti-Fogging solutions**

170 We first examined different ratios of carnauba and beeswax in two solvents namely  
171 Acetone and Ethanol to generate a homogenous solution (**Fig. 2A**). The contact angles of the  
172 acetone-based solutions were higher than their methanol counterparts (**Figs. 2B and 2C**). The  
173 coating with the highest contact angle was the 1: 2 ratio in acetone solution with a mean contact  
174 angle of  $150.3 \pm 2.1^\circ$ . This categorizes this surface coating as superhydrophobic and was  
175 significantly ( $p < 0.05$ ) more hydrophobic than the uncoated plastic surface. The higher  
176 concentrations at 1 : 2 ratio did not significantly improve these characteristics further. As expected  
177 the sliding angle for this coating was the lowest at  $13.7 \pm 2.1^\circ$  which was significantly ( $p < 0.05$ )  
178 lower than the uncoated plastic surface (**Figs. 2D and 2E**). The optical clarity of these formulation  
179 appears to vary with the concentration of the beeswax component as lower amounts resulted in  
180 higher clarity (**Figs. 2F and 2G**). The methanol-based formulations had a higher degree of optical  
181 clarity than the acetone counterparts. Based on these results, we decided to pursue the 1:2 carnauba  
182 to bee wax in acetone formulation for subsequent studies.

### 183 **Effect of routine disinfection procedures on durability of antifogging solution**

184 The use of disinfectants is a necessary part of routine plastic mask and face shield due to  
185 the prominent aerosol generating dental procedures. (33-35) Next, we examined routine  
186 disinfectant procedures employed in the dental office namely, soapy water, 70% Isopropyl Alcohol  
187 with paper towels, gauze, or microfiber, and disinfectant wipes. We noted a significant ( $p < 0.05$ )  
188 reduction in the contact angle after all disinfection methods (**Fig. 3A**). Among all these methods,  
189 Isopropyl Alcohol with gauze reduced the contact angle the least ( $144.3 \pm 1.6^\circ$ ) while soap made

190 the surface most hydrophilic (wetable). Concurrently, the sliding angle analysis showed a similar  
191 trend, increasing overall with all, but the soap group, disinfection methods (**Fig. 3B**). The Isopropyl  
192 alcohol group showed the least change and no statistically significant difference was noted with  
193 the paper towel method. Interestingly, the optical clarity appeared to vary after individual  
194 disinfectant methods with some showing increases while other showing significant decreases (**Fig.**  
195 **3C**). The method of disinfection that showed most increase in light transmission was wipes alone  
196 while the most reduction was observed with Isopropyl Alcohol and paper towel method. These  
197 results suggest that using Isopropyl Alcohol with gauze is optimal for disinfection as it minimally  
198 affects antifogging coating properties after repeated use.

### 199 **Antifogging coating stability after contact wear testing**

200 Finally, we investigated the durability of the anti-fogging solutions as they would be  
201 subjected to rigorous daily wear and tear during PPE use. We first created a simple rig to simulate  
202 skin contact based on a 3D printed apparatus (**Fig. 4A and B**). The rig was designed as a rotating  
203 platform that would result in a repetitive contact of the coated device with a stationary leather  
204 surface. The force exerted by facemask on the nose bridge and chin contact has been assessed to  
205 be 45 to 91 mm of Hg (6000-12,000 N/m<sup>2</sup>) (**Fig. 4C**). (30-32) The constant skin contact force in  
206 our device was assessed to be 5000 N/m<sup>2</sup> that could be approximated to a repeated light skin  
207 contact.

208 Following the simulated wear, the contact and sliding angle as well as optical clarity was  
209 assessed. We observed a significant ( $p < 0.05$ ) reduction in contact angle ( $133.3 \pm 1.5^\circ$ ) and  
210 concomitant increase in the sliding angle ( $23.7 \pm 1.5^\circ$ ) compared to the uncoated control surfaces.  
211 While optical clarity was not significantly different before and after wear simulation, there was a  
212 trend towards reduced transmission. Ultrastructure analysis noted the wear simulation resulted in  
213 significant accretions and scratches that likely contribute to the reduced light transmission  
214 observed. These results indicate the coating will likely need to be replaced over repeated PPE use  
215 as often as every other week.

216

217

218

219

220

221 **DISCUSSION**

222           The COVID pandemic presented new challenges to healthcare with an urgent need for  
223 innovations in disinfection approaches. The use of PPEs was central in the attempts to mitigate the  
224 spread of infection and a major part of the solution to mitigate the health crisis. The use of these  
225 barriers continues to have an impact on both the psychological, and medical well-being of both the  
226 patients and the healthcare professionals themselves.(36) The initial response to the pandemic  
227 brought manufacturing and supply chain disruptions resulting in additive 3D printing enthusiasts  
228 to offer custom, local solutions. Our team at the University at Buffalo focused on the transparent  
229 PPE designs and dental loop attachments as our innovative solution. The condensation from  
230 breathing obscured the functions of the clear PPEs that presented a major impasse to their use.  
231 This work was specifically motivated to address this deterrent for routine clear PPE use.

232           We tested two transparent polymers for this analysis namely Polyvinyl chloride (PVC) and  
233 polyethylene terephthalate glycol (PETG). PETG is a thermoplastic that has a reputation for its  
234 high impact resistance and ductility, offers better chemical resistance and durability, and is  
235 commonly used. To generate an anti-fogging solution for our clear face shields and masks, a major  
236 design challenge was the close proximity to nose and mouth.(37,38) We chose to pursue natural  
237 waxes as the main ingredient as they provided a natural, non-toxic solution that has a well-  
238 established track record of biological safety. (39) The other major component constituent was an  
239 polar solvent to enhance miscibility and dispersion of these waxes. We chose to examine Acetone  
240 and Ethanol in our formulation. The Acetone formulation performed more superiorly to generate  
241 the most superhydrophobic product for spray coating. Our initial efforts at dissolving the waxes in  
242 Acetone (boiling point of 132.8°F) by heating alone resulted in evaporation and non-uniform  
243 dissolution. Hence, we chose to utilize ultrasonication that resulted in an effective homogenous  
244 solution. Among the various formulations, the most superhydrophobic surface was generated by  
245 the 1 : 2 ratio (contact angle  $150.3 \pm 2.1^\circ$ ) while other formulations were also hydrophobic (contact  
246 angles 121 to 135°). We also examined Methanol (boiling point of 148.5 °F) in the same volume  
247 that, in contrast, generated hydrophilic surface coatings with all formulations (contact angles 34 to  
248 82 °), but most prominently with the 1: 2 at the higher concentration (contact angle  $80.7 \pm 2.1^\circ$ ).

249 Among the two solvents examined, Methanol did not enable a suitable anti-fogging formulation  
250 and hence, the 1: 2 formulation in Acetone was chosen as an optimal anti-fogging solution.

251 The use of surface disinfectants is an integral part of maintaining and reusing PPEs. This  
252 is a sustainable and cost-effective practice that is routinely employed. A key design requirement  
253 of the anti-fogging solution is durability with these disinfectant approaches. We observed that the  
254 soap solution group consistently demonstrated complete removal of the anti-fogging solution.  
255 While this desirable as a disinfectant approach to remove all potentially hazardous aerosols on  
256 these PPEs, it would not be suitable with the applied anti-fogging solution. The removal of the  
257 anti-fogging solution with these approaches could be attributed to the surfactant nature that  
258 interferes with the surface tension of the water droplets. Another possibility is that the lipid-to-  
259 lipid interaction of the soap and the waxes may inactivate the hydrophobic nature of the coating.  
260 These remain to be investigated in future studies.

261 To investigate the durability of the anti-fogging coating, we generated a custom rig for  
262 accelerated surface contact testing. The major design principle for this device was to generate a  
263 PPE skin contact force. The reported PPE skin contact force to create a tight seal on the nose and  
264 chin has been reported as 45 to 91 mm of Hg (6000-12,000 N/m<sup>2</sup>). (30-32) The force generated by  
265 our rig was a little lower at 5000 N/m<sup>2</sup> that approximates light skin contact force in non-fastened  
266 areas. This reflects routine surface contact during routine use of the PPEs. The integrity of the anti-  
267 fogging surfaces was relatively well maintained (contact angle  $133.3 \pm 1.5^\circ$  and sliding angle  $23.7$   
268  $\pm 1.5^\circ$ ). However, the durability testing noted a reduction in the optical clarity of the masks that  
269 could be attributed the wear from the contact forces. As evident in the ultrastructural analysis, the  
270 PETG surface appears to have several accretions and disruption of the uniform coated surfaces.  
271 Given these PPEs are disposable and have a limited time of use, this may not significantly impact  
272 the PPE performance. In fact, this lack of clarity from routine use may be a good marker for  
273 replacement with a simple optical interferometry device.

274 This study has a few limitations. First, the biological performance of this anti-fogging  
275 solution needs to be validated using *in vitro* (reconstructed human epidermis), and *in vivo* skin  
276 contact testing in animals and human studies. (40-46) Second, applying a superhydrophobic  
277 solution on the PETG clear surface may, counter to its primary objective, worsen the visibility due  
278 to the moisture coalescing into larger water beads. It is conceivable that the increasing size of these

279 water beads may eventually reach a critical mass and cause them to slide off. This phenomenon is  
280 observed on the lotus leaves and commercial car wax coatings. Hence, a replaceable absorbent  
281 liner and a mild, mechanical vibration module to promote water droplet beading and run-off could  
282 be future design iteration in these clear PPEs. Third, a major shortcoming of using such an anti-  
283 fogging spray is its temporary nature and the need for continuous replacement throughout the  
284 lifetime of the clear PPE. Thus, a potential future possibility is to pursue nanopatterning,  
285 simulating the lotus leaf papillae for a more biocompatible, permanent anti-fogging solution.

## 286 **Conclusions**

287 In summary, this work demonstrates the utility of an anti-fogging formulation with two  
288 natural waxes that has good durability and optimal non-fouling properties. This solution appears  
289 to represent a cost-effective, durable, non-toxic approach to prevent or reduce fogging of clear  
290 PPEs such as plastic masks and face shields from condensations during humidity natural breathing  
291 and speaking.

292

## 293 **Acknowledgements**

294 We thank the members of the Buffalo3DPPE for their time and effort during the pandemic namely,  
295 Kierra Bleyle, Preethi Singh, Jason Ciano, Savannah Tomaka, Jacob Graca, Hunter Rosa, Yianni  
296 Savidis, Danielle Detwiler, Omer Hillel, and Georgia Kyriacou. We also thank the Buffalo Enable  
297 (BE Mask) team for their valuable collaboration and technical assistance with 3D printing namely  
298 Aaron Gorsline, Albert Titus, Ben Rubin, Kelly Cheatle, James Whitlock, Jeremy Simon, Jon  
299 Schull, Pete Suffoletto, Peter Elkin, and Skip Meetze. We thank Mr. Peter Bush, South Campus  
300 Instrument core for assisting with the SEM analysis. We thank the University at Buffalo, BlueSky,  
301 and Dean's fund, School of Dental Medicine for funding this project.

302

## 303 **Conflicts of Interests**

304 The authors declare they have no relevant conflicts of interest with this work.

305

306 **References**

- 307 1. Pak A, Adegboye OA, Adekunle AI, Rahman KM, McBryde ES, Eisen DP. Economic Consequences  
308 of the COVID-19 Outbreak: the Need for Epidemic Preparedness. *Front Public Health* 2020; 8:241.
- 309 2. Pirasteh-Anosheh H, Parnian A, Spasiano D, Race M, Ashraf M. Haloculture: A system to mitigate  
310 the negative impacts of pandemics on the environment, society and economy, emphasizing  
311 COVID-19. *Environ Res* 2021; 198:111228.
- 312 3. Goriuc A, Sandu D, Tatarciuc M, Luchian I. The Impact of the COVID-19 Pandemic on Dentistry and  
313 Dental Education: A Narrative Review. *Int J Environ Res Public Health* 2022; 19(5).
- 314 4. Kurian N, Gandhi S, Thomas AM. COVID-19 and multidisciplinary dentistry. *Br Dent J* 2021;  
315 231(9):534.
- 316 5. Lieberthal B, McCauley LK, Feldman CA, Fine DH. COVID-19 and Dentistry: Biological  
317 Considerations, Testing Strategies, Issues, and Regulations. *Compend Contin Educ Dent* 2021;  
318 42(6):290-296; quiz 297.
- 319 6. Artenstein AW. In Pursuit of PPE. *N Engl J Med* 2020; 382(18):e46.
- 320 7. Marcus K, Balasubramanian M, Short SD, Sohn W. Dental hesitancy: a qualitative study of  
321 culturally and linguistically diverse mothers. *BMC Public Health* 2022; 22(1):2199.
- 322 8. Muneer MU, Ismail F, Munir N, Shakoor A, Das G, Ahmed AR, Ahmed MA. Dental Anxiety and  
323 Influencing Factors in Adults. *Healthcare (Basel)* 2022; 10(12).
- 324 9. Nikolic M, Mitic A, Petrovic J, Dimitrijevic D, Popovic J, Barac R, Todorovic A. COVID-19: Another  
325 Cause of Dental Anxiety? *Med Sci Monit* 2022; 28:e936535.
- 326 10. Blais C, Fiset D, Roy C, Saumure Regimbald C, Gosselin F. Eye fixation patterns for categorizing  
327 static and dynamic facial expressions. *Emotion* 2017; 17(7):1107-1119.
- 328 11. Chodosh J, Weinstein BE, Blustein J. Face masks can be devastating for people with hearing loss.  
329 *BMJ* 2020; 370:m2683.
- 330 12. Chu JN, Collins JE, Chen TT, Chai PR, Dadabhoy F, Byrne JD, Wentworth A, DeAndrea-Lazarus IA,  
331 Moreland CJ, Wilson JAB, Booth A, Ghenand O, Hur C, Traverso G. Patient and Health Care Worker  
332 Perceptions of Communication and Ability to Identify Emotion When Wearing Standard and  
333 Transparent Masks. *JAMA Netw Open* 2021; 4(11):e2135386.
- 334 13. Fleming JT, Maddox RK, Shinn-Cunningham BG. Spatial alignment between faces and voices  
335 improves selective attention to audio-visual speech. *J Acoust Soc Am* 2021; 150(4):3085.
- 336 14. MacLeod A, Summerfield Q. Quantifying the contribution of vision to speech perception in noise.  
337 *Br J Audiol* 1987; 21(2):131-141.
- 338 15. Schwartz JL, Berthommier F, Savariaux C. Seeing to hear better: evidence for early audio-visual  
339 interactions in speech identification. *Cognition* 2004; 93(2):B69-78.
- 340 16. Sonnichsen R, Llorach To G, Hochmuth S, Hohmann V, Radeloff A. How Face Masks Interfere With  
341 Speech Understanding of Normal-Hearing Individuals: Vision Makes the Difference. *Otol Neurotol*  
342 2022; 43(3):282-288.
- 343 17. Atcherson SR, Mendel LL, Baltimore WJ, Patro C, Lee S, Pousson M, Spann MJ. The Effect of  
344 Conventional and Transparent Surgical Masks on Speech Understanding in Individuals with and  
345 without Hearing Loss. *J Am Acad Audiol* 2017; 28(1):58-67.
- 346 18. Belhouideg S. Impact of 3D printed medical equipment on the management of the Covid19  
347 pandemic. *Int J Health Plann Manage* 2020; 35(5):1014-1022.
- 348 19. O'Connor S, Mathew S, Dave F, Tormey D, Parsons U, Gavin M, Nama PM, Moran R, Rooney M,  
349 McMorrow R, Bartlett J, Pillai SC. COVID-19: Rapid prototyping and production of face shields via  
350 flat, laser-cut, and 3D-printed models. *Results Eng* 2022; 14:100452.

- 351 20. Rupesh Kumar J, Mayandi K, Joe Patrick Gnanaraj S, Chandrasekar K, Sethu Ramalingam P. A  
352 critical review of an additive manufacturing role in Covid-19 epidemic. *Mater Today Proc* 2022;  
353 68:1521-1527.
- 354 21. Vallatos A, Maguire JM, Pilavakis N, Cerniauskas G, Sturtivant A, Speakman AJ, Gourlay S, Inglis S,  
355 McCall G, Davie A, Boyd M, Tavares AAS, Doherty C, Roberts S, Aitken P, Mason M, Cummings S,  
356 Mullen A, Paterson G, Proudfoot M, Brady S, Kesterton S, Queen F, Fletcher S, Sherlock A, Dunn  
357 KE. *Adaptive Manufacturing for Healthcare During the COVID-19 Emergency and Beyond*. *Front*  
358 *Med Technol* 2021; 3:702526.
- 359 22. Kalkal A, Allawadhi P, Kumar P, Sehgal A, Verma A, Pawar K, Pradhan R, Paital B, Packirisamy G.  
360 Sensing and 3D printing technologies in personalized healthcare for the management of health  
361 crises including the COVID-19 outbreak. *Sens Int* 2022; 3:100180.
- 362 23. Arany PSaP. *Dental Faceshields*. 2020.
- 363 24. Laurén S. Contact angle measurements on superhydrophobic surfaces in practice. *Surface Science*  
364 *Blog: Biolin Scientific*; 2019.
- 365 25. Lv C, Yang C, Hao P, He F, Zheng Q. Sliding of water droplets on microstructured hydrophobic  
366 surfaces. *Langmuir* 2010; 26(11):8704-8708.
- 367 26. Razavi SMR OJ, Sett S, et al. Superhydrophobic Surfaces Made from Naturally Derived  
368 Hydrophobic Materials. *ACS Sustainable Chem Eng* 2016.
- 369 27. Bormashenko E. Wetting of real solid surfaces: new glance on well-known problems. *Colloid and*  
370 *Polymer Science* 2013.
- 371 28. Li P. Submillimeter Papillae: Shape Control of Lotus Leaf Induced by Surface Submillimeter  
372 Texture. *Advanced Materials Interfaces* 2020.
- 373 29. Wang P QX, Shen J. Superhydrophobic Coatings with Edible Biowaxes for Reducing or Eliminating  
374 Liquid Residues of Foods and Drinks in Containers. *Bioresources* 2018.
- 375 30. Brill AK, Pickersgill R, Moghal M, Morrell MJ, Simonds AK. Mask pressure effects on the nasal  
376 bridge during short-term noninvasive ventilation. *ERJ Open Res* 2018; 4(2).
- 377 31. Dellweg D, Hochrainer D, Klauke M, Kerl J, Eiger G, Kohler D. Determinants of skin contact pressure  
378 formation during non-invasive ventilation. *J Biomech* 2010; 43(4):652-657.
- 379 32. Schettino GP, Tucci MR, Sousa R, Valente Barbas CS, Passos Amato MB, Carvalho CR. Mask  
380 mechanics and leak dynamics during noninvasive pressure support ventilation: a bench study.  
381 *Intensive Care Med* 2001; 27(12):1887-1891.
- 382 33. Epstein JB, Chow K, Mathias R. Dental procedure aerosols and COVID-19. *Lancet Infect Dis* 2021;  
383 21(4):e73.
- 384 34. Mick P, Murphy R. Aerosol-generating otolaryngology procedures and the need for enhanced PPE  
385 during the COVID-19 pandemic: a literature review. *J Otolaryngol Head Neck Surg* 2020; 49(1):29.
- 386 35. Wilson NM, Norton A, Young FP, Collins DW. Airborne transmission of severe acute respiratory  
387 syndrome coronavirus-2 to healthcare workers: a narrative review. *Anaesthesia* 2020; 75(8):1086-  
388 1095.
- 389 36. Kisielinski K, Giboni P, Prescher A, Klosterhalfen B, Graessel D, Funken S, Kempfski O, Hirsch O. Is a  
390 Mask That Covers the Mouth and Nose Free from Undesirable Side Effects in Everyday Use and  
391 Free of Potential Hazards? *Int J Environ Res Public Health* 2021; 18(8).
- 392 37. Rothe H, Fautz R, Gerber E, Neumann L, Rettinger K, Schuh W, Gronewold C. Special aspects of  
393 cosmetic spray safety evaluations: principles on inhalation risk assessment. *Toxicol Lett* 2011;  
394 205(2):97-104.
- 395 38. Tha EL, Canavez A, Schuck DC, Gagosian VSC, Lorencini M, Leme DM. Beyond dermal exposure:  
396 The respiratory tract as a target organ in hazard assessments of cosmetic ingredients. *Regul*  
397 *Toxicol Pharmacol* 2021; 124:104976.

- 398 39. Final Report on the Safety Assessment of Candelilla Wax, Carnauba Wax, Japan Wax, and  
399 Beeswax. *J Am Coll Toxicol* 1984; 3(3).
- 400 40. Arnesdotter E, Rogiers V, Vanhaecke T, Vinken M. An overview of current practices for regulatory  
401 risk assessment with lessons learnt from cosmetics in the European Union. *Crit Rev Toxicol* 2021;  
402 51(5):395-417.
- 403 41. Choksi NY, Truax J, Layton A, Matheson J, Mattie D, Varney T, Tao J, Yozzo K, McDougal AJ, Merrill  
404 J, Lowther D, Barroso J, Linke B, Casey W, Allen D. United States regulatory requirements for skin  
405 and eye irritation testing. *Cutan Ocul Toxicol* 2019; 38(2):141-155.
- 406 42. Filaire E, Nachat-Kappes R, Laporte C, Harmand MF, Simon M, Poinot C. Alternative in vitro  
407 models used in the main safety tests of cosmetic products and new challenges. *Int J Cosmet Sci*  
408 2022; 44(6):604-613.
- 409 43. Hardwick RN, Betts CJ, Whritenour J, Sura R, Thamsen M, Kaufman EH, Fabre K. Drug-induced skin  
410 toxicity: gaps in preclinical testing cascade as opportunities for complex in vitro models and  
411 assays. *Lab Chip* 2020; 20(2):199-214.
- 412 44. Nabarretti BH, Rigon RB, Burga-Sanchez J, Leonardi GR. A review of alternative methods to the  
413 use of animals in safety evaluation of cosmetics. *Einstein (Sao Paulo)* 2022; 20:eRB5578.
- 414 45. Pistollato F, Madia F, Corvi R, Munn S, Grignard E, Painsi A, Worth A, Bal-Price A, Prieto P, Casati S,  
415 Berggren E, Bopp SK, Zuang V. Current EU regulatory requirements for the assessment of  
416 chemicals and cosmetic products: challenges and opportunities for introducing new approach  
417 methodologies. *Arch Toxicol* 2021; 95(6):1867-1897.
- 418 46. Riebeling C, Luch A, Tralau T. Skin toxicology and 3Rs-Current challenges for public health  
419 protection. *Exp Dermatol* 2018; 27(5):526-536.

420

421

422

423

424

425

426

427

428

429

430

431

## 432 **Figure Legends**

### 433 **Figure 1. Physical characterization of anti-fogging coating**

434 (A.) CAD of the contact angle apparatus for 3D printing (B.) CAD of the sliding angle module for  
435 3D printing (C.) 3D printed models of contact and sliding angle testing apparatus (D.) image of  
436 the contact angle assessment showing droplet generation and analysis. Inset shows the digital  
437 analysis of contact angle  $\phi$  using NIH ImageJ (E.) Digital image analysis showing the sliding angle  
438 measurement using NIH ImageJ (F.) Optical clarity set-up using a diode laser and optical power  
439 meter with sensor.

### 440 **Figure 2. Anti-fogging solution formulation and characterization**

441 (A.) Tabular outline of the formulation depicting ratios of carnauba and beeswax in acetone and  
442 methanol used to coat PETG plastic sheets (B. and C.) Contact angle assessment of Acetone and  
443 Methanol formulations at various concentrations (D and E) Sliding angle analysis of Acetone and  
444 Methanol formulations at various concentrations (F and G) Transmission of diode laser for optical  
445 clarity assessment of Acetone and Methanol formulations at various concentrations. Data is shown  
446 as Mean and SD and is representative of at least two independent studies. Statistical significance  
447 was determined using two-way analysis of variance (ANOVA) among different treatments using  
448 the Bonferroni's multiple comparison test ( $n = 3$ ). Statistical significance is denoted as \*  $p < 0.05$ ,  
449 \*\*  $p < 0.005$ , and \*\*\*  $p < 0.0005$ .

### 450 **Figure 3. Effects of Disinfection on anti-fogging coating integrity**

451 (A.) Contact angle assessment after various disinfection procedures (B.) Sliding angle analysis  
452 after various disinfection procedures (C.) Optical clarity after various disinfection procedures.  
453 Data is shown as Mean and SD and is representative of at least two independent studies. Statistical  
454 significance was determined using two-way analysis of variance (ANOVA) among different  
455 treatments using the Bonferroni's multiple comparison test ( $n = 3$ ). Statistical significance is  
456 denoted as \*  $p < 0.05$ , \*\*  $p < 0.005$ , \*\*\*  $p < 0.0005$ , and \*\*\*\*  $p < 0.00005$ .

### 457 **Figure 4. Durability testing of anti-fogging coating following contact testing**

458 (A.) CAD of contact testing apparatus used for wear testing analysis (B.) 3D printed model of the  
459 assembled contact testing apparatus (C.) Outline of the eminent forces determining the contact

460 force on PETG surfaces. The contact angle (**D.**), sliding angle (**E.**), and optical clarity (**F.**) analysis  
461 before and after contact testing (**G.**) Scanning electron microscopy images of the uncoated and  
462 coated surfaces before and after contact testing. Data is shown as Mean and SD and is  
463 representative of atleast two independent studies. Statistical significance was determined using  
464 Student T test ( $n = 3$ ). Statistical significance is denoted as \*  $p < 0.05$ .

465

466

# Figure 1

Figure 1. Physical characterization of anti-fogging coating

(**A.**) CAD of the contact angle apparatus for 3D printing (**B.**) CAD of the sliding angle module for 3D printing (**C.**) 3D printed models of contact and sliding angle testing apparatus (**D.**) image of the contact angle assessment showing droplet generation and analysis. Inset shows the digital analysis of contact angle  $\phi$  using NIH ImageJ (**E.**) Digital image analysis showing the sliding angle measurement using NIH ImageJ (**F.**) Optical clarity set-up using a diode laser and optical power meter with sensor.

Fig. 1

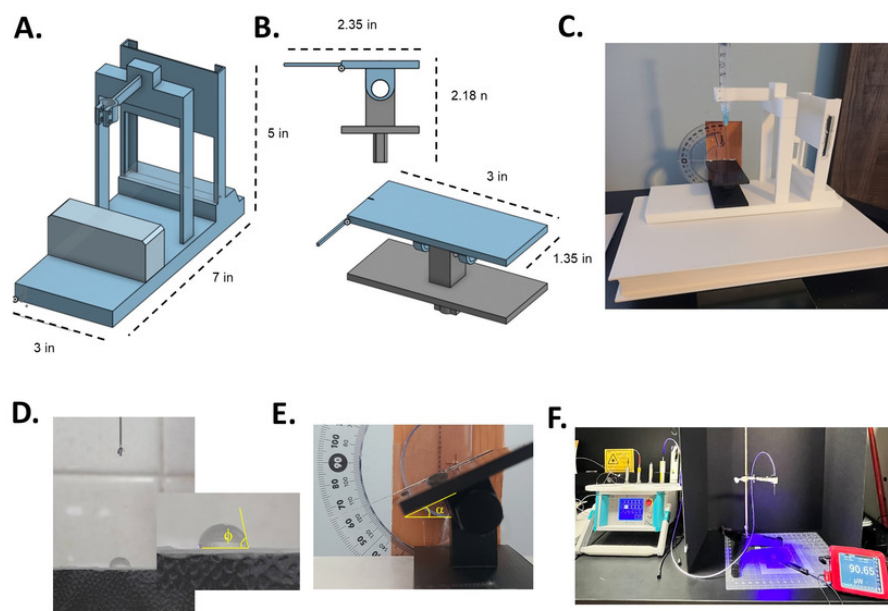


## Figure 2

### Figure 2. Anti-fogging solution formulation and characterization

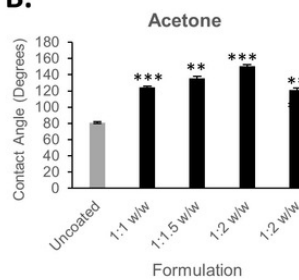
**(A.)** Tabular outline of the formulation depicting ratios of carnauba and beeswax in acetone and methanol used to coat PETG plastic sheets **(B. and C.)** Contact angle assessment of Acetone and Methanol formulations at various concentrations **(D and E)** Sliding angle analysis of Acetone and Methanol formulations at various concentrations **(F and G)** Transmission of diode laser for optical clarity assessment of Acetone and Methanol formulations at various concentrations. Data are shown as Mean and SD and representative of at least two independent studies. Statistical significance was determined using two-way analysis of variance (ANOVA) among different treatments using Bonferroni's multiple comparison test ( $n = 3$ ). Statistical significance is denoted as \*  $p < 0.05$ , \*\*  $p < 0.005$ , and \*\*\*  $p < 0.0005$ .

Fig. 2

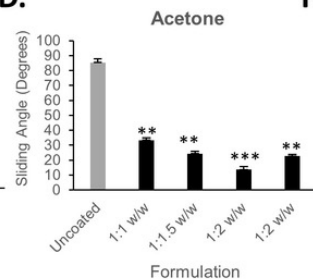
A.

Ratio	Carnauba (g)	Beeswax (g)	Acetone/Methanol (ml)
1:1	0.4375	0.4375	25
1:1.5	0.35	0.525	25
1:2	0.33	0.67	25
1:2 (HC)	0.417	0.833	25

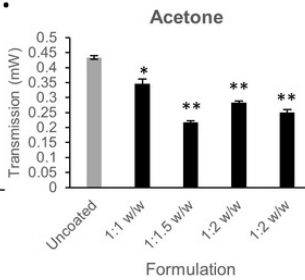
B.



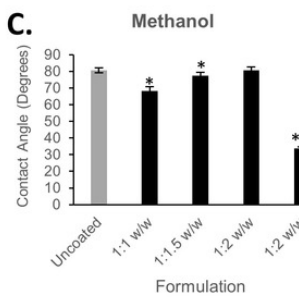
D.



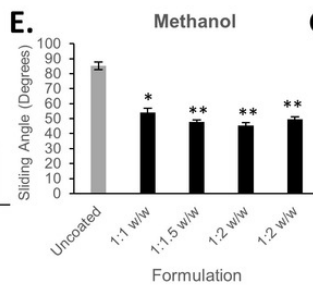
F.



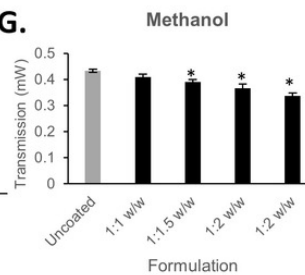
C.



E.



G.



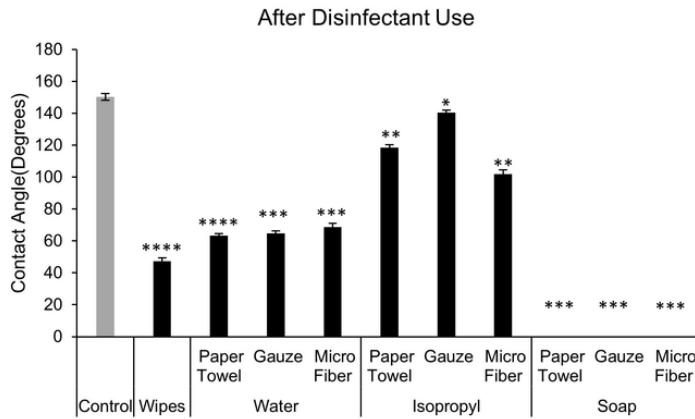
## Figure 3

Figure 3. Effects of Disinfection on anti-fogging coating integrity

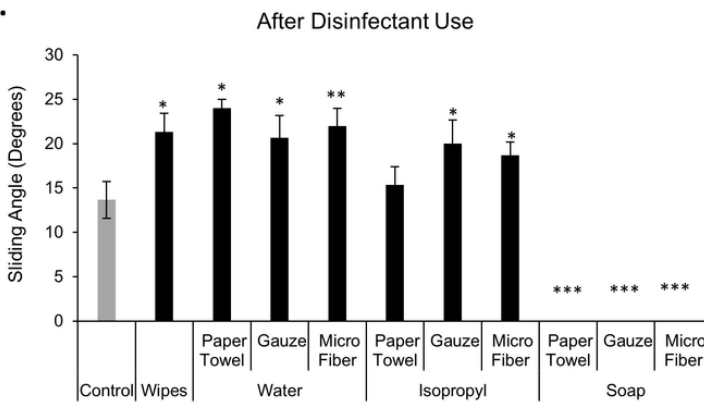
**(A.)** Contact angle assessment after various disinfection procedures **(B.)** Sliding angle analysis after various disinfection procedures **(C.)** Optical clarity after various disinfection procedures. Data are shown as Mean and SD and representative of at least two independent studies. Statistical significance was determined using two-way analysis of variance (ANOVA) among different treatments using Bonferroni's multiple comparison test ( $n = 3$ ). Statistical significance is denoted as \*  $p < 0.05$ , \*\*  $p < 0.005$ , \*\*\*  $p < 0.0005$ , and \*\*\*\*  $p < 0.00005$ .

Fig. 3

A.



B.



C.

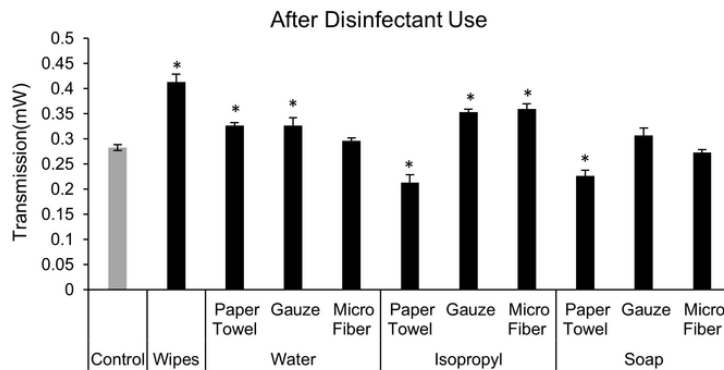


## Figure 4

Figure 4. Durability testing of anti-fogging coating following contact testing

(**A.**) CAD of contact testing apparatus used for wear testing analysis (**B.**) 3D printed model of the assembled contact testing apparatus (**C.**) Outline of the eminent forces determining the contact force on PETG surfaces. The contact angle (**D.**), sliding angle (**E.**), and optical clarity (**F.**) analysis before and after contact testing (**G.**) Scanning electron microscopy images of the uncoated and coated surfaces before and after contact testing. Data are shown as Mean and SD and representative of at least two independent studies. Statistical significance was determined using the Students' T-test ( $n = 3$ ). Statistical significance is denoted as \*  $p < 0.05$ .

Fig. 4

